Pure Appl. Chem., Vol. 80, No. 11, pp. 2439–2449, 2008.
doi:10.1351/pac200880112439

In situ transient study of polymer film growth via simultaneous correlation of charge, mass, and ellipsometric measurements*

Vojtech Svoboda and Bor Yann Liaw‡

Hawaii Natural Energy Institute, School of Ocean and Earth Science and Technology, University of Hawaii at Manoa, 1680 East-West Road, POST 109, Honolulu, HI 96822, USA

Abstract: Using three synchronized, in situ, nonintrusive, real-time characterization techniques to conduct transient observations, we revealed mechanistic details of a polymer film growth. A thin methylene green (MG) polymer coating (of the order of 35 nm) was used as a model system in this electrochemical microgravimetric imaging ellipsometry (EmIE) investigation. The direct correlation of changes in mass (via quartz crystal microbalance, QCM), ellipsometric angles (via imaging ellipsometry) with electrochemical conditions (in cyclic voltammetry, CV) provides discrete temporal and spatial information to help us decipher the underlying steps, from which we were able to separate adsorption, reduction, oxidation, desorption, and polymerization regimes involved in the deposition process. The evidence revealed in this study could have broad impact on the general understanding regarding how a film is deposited onto a metal surface.

Keywords: in situ; mass-charge-ellipsometric angle correlation; transient; imaging ellipsometry; QCM; cyclic voltammetry.

INTRODUCTION

Controlling deposition of redox polymer films has been an interesting subject of study in the past decades [1–14], primarily because of their potential applications in either passive (e.g., for corrosion protection) or conductive (e.g., for energy conversion/storage systems or electronics) forms. The rapid expansion of interests in nanomaterials and fabrications demands better temporal and spatial characterization techniques to facilitate research and development. However, only a few nano- or mesoscale characterization techniques (such as atomic force microscopy (AFM); e.g., [15–17]) are available for in situ observations, particularly in solutions. In addition, few can easily allow any moderate to large area observation with respect to transient experimental conditions. Thus, any in situ, nonintrusive technique to offer such a utility appears very attractive, especially for surface or interface characterizations in liquid environments.

Quartz crystal microbalance (QCM) can measure nanograms of mass change on an electrode surface [18]. The availability of imaging ellipsometry [19–21] not only allows the measurements of ellipsometric angles, which can be used for determination of film thickness down to nanoscales but also per-

*Paper based on a presentation at the 3rd International Symposium on Novel Materials and Their Synthesis (NMS-III) and the 17th International Symposium on Fine Chemistry and Functional Polymers (FCFP-XVII), 17–21 October 2007, Shanghai, China. Other presentations are published in this issue, pp. 2231–2563.

‡Corresponding author: Tel.: (808) 956-2339; Fax: (808) 956-2336; E-mail: bliaw@hawaii.edu

mits the observations of surface morphology and roughness over a reasonably large viewing area. Electrochemical techniques such as cyclic voltammetry (CV) are often used for controlling and characterizing polymer depositions [22], which offer opportunities to study transient kinetics. Synchronically employing these three techniques in a single experiment provides us a very powerful tool to directly correlate simultaneously measured mass, charge, and film thickness evolutions in situ for observation of the dynamics in the polymer film growth and allows us to understand the kinetics involved in transient.

There have been numerous attempts in the past [1–14] to use various combinations of these in situ techniques (even with other spectroscopic techniques) to investigate film deposition and the resulting film properties. For example, Hamnett and Hillman used spectroscopic ellipsometry to study electrodeposition of polythionine and -thiophene [1,2] in solutions. They were able to calculate film composition and thickness with optical parameters (n, k) accounted for solvent ingress in the film development, thus fully explored the utility of the spectroscopic ellipsometry with electrochemical techniques. However, they did not use QCM to help them reap out the adsorption effect that should be accounted for in the optical model. Gottesfeld and coworkers [4–10] attempted to utilize various combinations of these techniques to study conjugated conductive polymers. For instance, they used all three techniques to explore the correlation of mass with film thickness in their study of electrochemical deposition of polyaniline films [5]. However, they did not study any transient complex redox reactions as we did in the CV, nor did they discuss any adsorption behavior that might incur in the system. The combined use of ellipsometry with QCM was later reported by others [11–14]. However, none of them has pursued direct correlation among mass, charge, and ellipsometric angles with temporal resolution in a transient, dynamic manner. In general, the ellipsometric angles not only change with the material's thickness but also reflect the material's optical, electrical, and other pertinent physical properties. The imaging ellipsometric technique is capable of probing evolutions of ellipsometric angles simultaneously with imaging to record the surface morphology development. Synchronously in company with nanoscale measurement of mass changes in relation to other experimental parameters and conditions, such as those imposed by electrochemical CV, we found this in situ, almost real-time combination of investigation capable of providing us a wealth of information that was not attainable before with other techniques. This information with detailed temporal and possibly spatial resolutions is a very useful tool to probe reaction kinetics much more than what has been offered by other techniques.

In this work, we use polymerization of methylene green (MG) as a model system to demonstrate the unique experimental utility of combining synchronized electrochemical, microgravimetric, and imaging ellipsometric measurements to study the poly-methylene green (poly-MG) film development in aqueous solution. We found that this in situ investigation with sufficient temporal resolution provides detailed information about the kinetics of the CV deposition process. Structural and chemical changes in the polymer (by redox reaction) are often associated with color change as well as with changes in electronic conductivity and dielectric constant. These changes directly reflect in the change of ellipsometric angles. We will explain how to use careful data analysis to derive the correlation among various pieces of information from different measurements to reach a coherent understanding of the stepwise processes involved in the film deposition. Such an analytical technique applied in situ in a kinetic measurement during CV, as we demonstrated in this paper, is a powerful tool; however, we must admit that with our single wavelength ellipsometer we were not able to make a quantitative analysis of the kinetic data. A multi-wavelength spectroscopic ellipsometry will enable us to conduct such quantitative analyses in the future.

EXPERIMENTAL

Reagents and materials

Analytical-grade MG was purchased from Sigma-Aldrich, Inc., (St. Louis, MO). Analytical-grade potassium nitrate (KNO_3), potassium phosphate monobasic (KH_2PO_4), and potassium phosphate dibasic (K_2HPO_4) were purchased from Fisher Scientific (Fairlawn, NJ). An MG deposition solution was made by dissolving MG and KNO_3 in 50 mM phosphate buffer (pH 7.0) to the final concentration of 0.1 mM MG and 0.1 M KNO_3. Phosphate buffer solution was made by mixing solutions of 0.05 M monobasic and dibasic potassium phosphates until the desired pH 7.0 was achieved. All solutions were made using 18 MΩ·cm ultra-pure water.

Before the experiment, the counter electrode was polished with 0.05 μm alumina powder and sonicated in 98 % methanol for 2 min then rinsed with 18 MΩ·cm ultra-pure water and air-dried. The working electrode was rinsed with methanol and then with 18 MΩ·cm ultra-pure water and air-dried.

Apparatus and instrumentation set-up

The polymerization of MG was conducted by a CV method in a three-electrode electrochemical cell assembly modified from a QCM crystal holder for FC-550 flow cell housing as a bottom piece, in which a Ti/Pt, AT-Cct, 5 MHz, QCM crystal optimized for 25 °C measurement (P/N 149274-1, f = 12.5 mm, Maxtek, Inc., Cypress, CA) was used. This crystal has a Ti adhesion layer (<100 nm) between the quartz crystal and the outer Pt electrode layer (~220 nm). The Pt surface is used as the working electrode in the experiment. The Pt layer of 220 nm is thick enough and works well as an ellipsometric substrate in our experiment without interference from the Ti underlayer. A stainless steel rod (f = 5.7 mm) was used as the counter electrode. A leak-free LF-2 Ag/AgCl (in 3.4 M KCl) electrode purchased from the Innovative Instruments, Inc. (Tampa, FL), was used as the reference. To construct the cell for in situ ellipsometric measurements, we used a top housing of a flow cell apparatus provided by Accurion Scientific Instruments (Menlo Park, CA) in combination with the Maxtek crystal holder housing and sealed by an o-ring (Fig. 1). The top housing has two optical windows that allow polarized incident laser beam (solid-state YAG source, 532 nm, 50 mW) to radiate on the sample surface direct and the reflected beam to reach the analyzer on the imaging ellipsometer (EP^3, also Accurion Scientific Instruments). The cell assembly has access ports to fill in solutions from a reservoir by a peristaltic pump or to degas the reaction chamber. The electrochemical deposition of the polymer was carried out by a Solartron Electrochemical Interface SI 1287 (Houston, TX). Since the ellipsometric and micrograviметric measurements are sensitive to temperature and mechanical vibration, the experiment was performed in a temperature-controlled environment and on an active vibration isolation platform (MOD-2S, Accurion Scientific Instruments).

The data collection and analysis was performed by each software application that controls the specific measurements in QCM (RQCM Data Logging Software V2.0.3, Maxtek), EP^3 (EP^3View V2.30, Accurion Scientific), and SI1287 (CorrWare-CorrView V.2.9b2, Scribner Associates, Southern Pines, NC), respectively. The mass change information was derived from the Sauerbrey equation [23] based on the frequency change measured from the resonance frequency of the quartz crystal electrode. The ellipsometric angles of the film were recorded and used directly from the measurements. The Δ and Ψ values can be used for determination of the poly-MG film thickness, which has been discussed elsewhere [24] and will not be repeated herein.

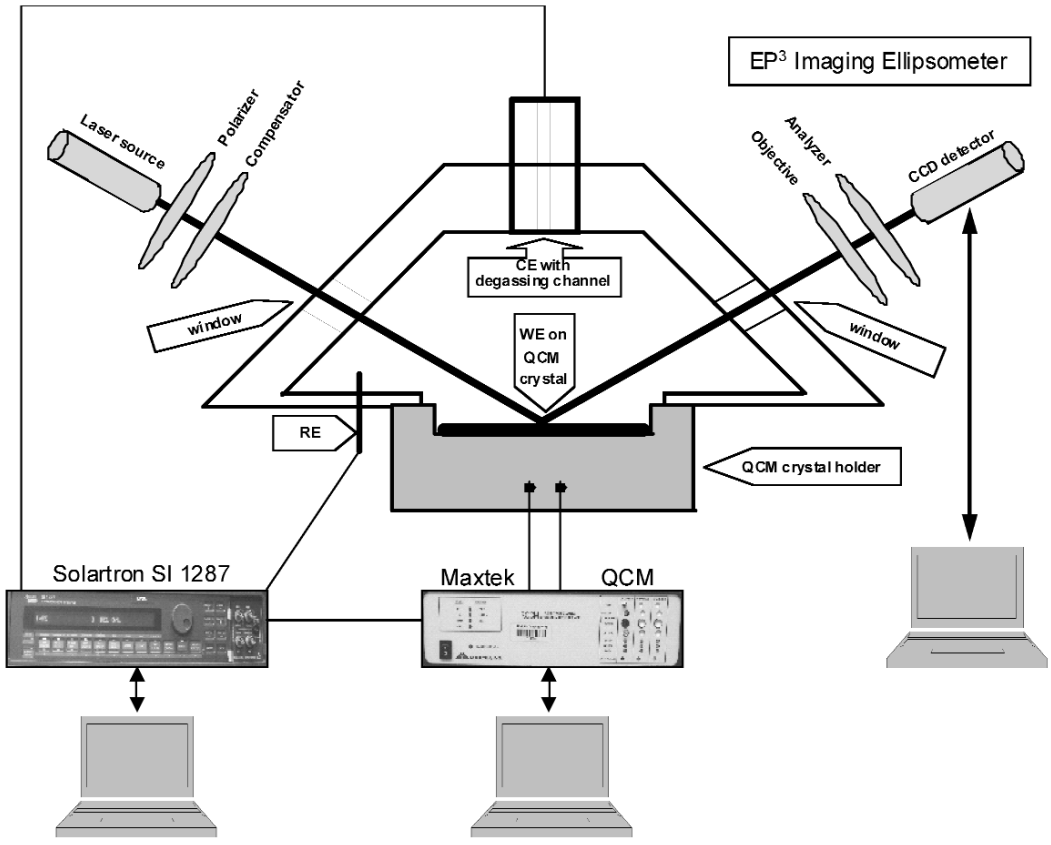

Fig. 1 Schematic of the experimental set-up of the EmIE with a three-electrode liquid cell for simultaneous mass, ellipsometric angles, and CV measurements.

Electrochemical polymerization of methylene green

The electrochemical cell was filled up and degassed by peristaltic pumping with 0.5 ml of MG solution. The poly-MG film was deposited by voltammetric cycling between –0.5 and +1.2 V vs. the reference at a sweep rate of $\nu = 10$ mV sec^{-1}. The low sweep rate was chosen primarily due to data acquisition limitation of the ellipsometer. The cycling started at –0.5 V (reduction) and was swept toward +1.2 V (oxidation) and swept back to the reduction ending at –0.5 V. In total, 16 cycles were performed. The data presented herein corresponds to the last four cycles (cycles 13–16). Cycle 14 was used explicitly to explain the correlation results.

RESULTS

Presentation of EmIE data

The most valuable merit of conducting synchronized electrochemical microgravimetric imaging ellipsometry (EmIE) experiment is to correlate changes in mass and geometric dimensions (primarily, the film thickness) via the reading from the ellipsometric angles directly with electrochemical deposition conditions. CV is used commonly to study electrode kinetics, and the results are usually presented in a current–voltage curve at a constant voltage sweep rate. The constant sweep rate allows us to translate the current–voltage curve into a current–time profile. To relate CV with the ellipsometric and microgravimetric data, we consider the most appropriate representation of the data is to correlate them both

in time and with voltage, so the sequence of events can be synchronized with reaction potential. In this manner, the variations in ellipsometric angles and mass in concert with the current will reveal the kinematics of the redox reactions taking place on the electrode surface. In other words, the first derivative of the mass and ellipsometric angle vs. time profiles, which represents the rate of change in mass and film thickness with time, will be correlated with the change of electrical charge reacted on the electrode surface.

Cyclic voltammetry

The voltammograms of cycles 13–16 of poly-MG deposition are shown in Fig. 2. In the forward sweep from 1.2 to –0.5 V, a reduction peak 1 was observed at –0.42 V vs. Ag AgCl. In the backward sweep, an oxidation peak 2 was expected between –0.2 and 0.2 V [25]. At 10 mV s^{-1} we did not observe this oxidation peak. However, a small anodic peak was observed [24] at a sweep rate of 50 mV/s^{-1}. We have observed some difference in voltammograms between Pt surface [24] and glassy carbon [26] due to surface preparation and kinetics. Reaction 3 (from 0.6 to 1.2 V) corresponds to the MG polymerization on the electrode.

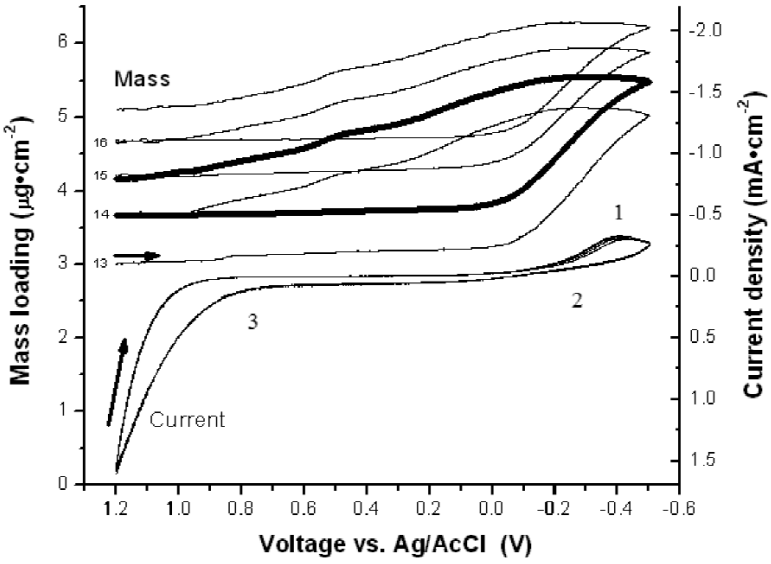

Fig. 2 CV with QCM mass excursion profiles. The curve in bold is cycle 14. The arrows indicate the direction of voltage sweep (in time propagation).

Microgravimetry

The progression of mass (m) change in cycles 13–16 (cycle 14 in bold) is shown in Fig. 2 above with the CVs. Figure 3 displays the progression of mass, current, and dm/dt of cycle 14. In the forward sweep toward –0.5 V, the mass began to increase in a rapidly progressive manner when the potential passed 0.2 V toward the negative. The mass change rate dm/dt reaches the maximum ("M1" in Fig. 3) at about –0.28 V. In contrast, the reduction current reaches the peak at –0.42 V (peak 1 in Fig. 3). The maximum cumulative mass ("MM" in Fig. 3) is achieved in the backward sweep after the reduction current peak.

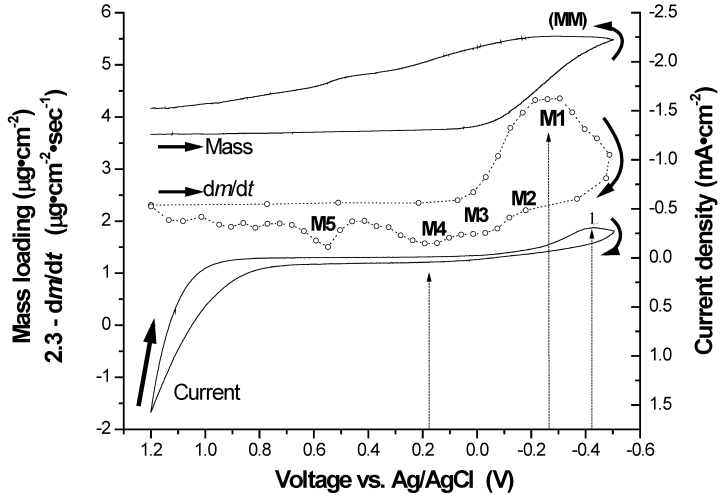

Fig. 3 CV with the QCM mass excursion profile of cycle 14, and the derivative d*m*/d*t*. The arrows indicate the direction of voltage sweep (in time propagation).

Ellipsometry

The progression of ellipsometric angle delta (Δ) along with the current and dΔ/d*t* profiles in cycle 14 is shown in Fig. 4. In the beginning of the cycle, as the forward sweep moves toward the reduction regime, the parameter Δ remains practically constant until the potential approaches 0.2 V and onward to negative. In the subsequent reduction regime, the Δ rapidly increases. The rate of increase dΔ/d*t* reaches the maximum (D1 in Fig. 4) at –0.245 V. As the Δ continues to increase, surpassing the reduction current peak, it reaches the maximum in the backward sweep at –0.31 V, where dΔ/d*t* = 0.

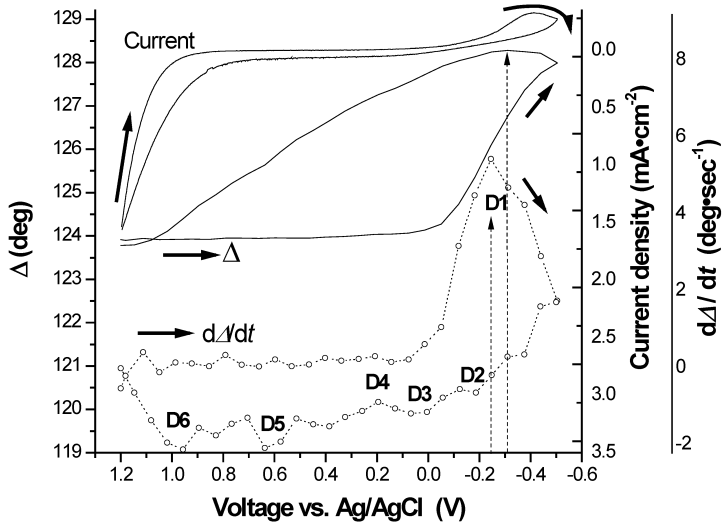

Fig. 4 Progression of ellipsometric angle Δ during CV sweep and dΔ/d*t* of cycle 14. The arrows indicate the direction of voltage sweep (in time propagation).

The progression of the ellipsometric angle Ψ in cycle 14 is shown in Fig. 5, along with the current and dΨ/dt profiles. In the forward sweep (from 1.2 to 0.9 V), the dΨ/dt slightly decreases, and then remains constant until the potential sweeps to negative in the reduction regime. The dΨ/dt rapidly increases from the onset near 0.2 V, which coincides with the onset of dm/dt. The dΨ/dt exhibits two peaks, P1a and P1b, in this reduction regime. The peak P1a is located near the same potential as the M1 peak, while P1b coincides with the reduction peak 1. The Ψ profile reaches the maximum at –0.44 V in the backward sweep, which coincides with P1b, followed by a progressive Ψ decrease. A change in the slope of dΨ/dt was observed at P2, which may signal a shift in the nature of the underlying process. At P3 (at +0.07 V), the largest decrease in dΨ/dt was recorded. After this point, Ψ decrease decelerated. This trend deflected at +0.26 V (P4). The dΨ/dt between P3 and P4 followed the development of the dm/dt and dΔ/dt profiles. In the subsequent oxidation regime, we observed a peak P5 at +0.58 V. This peak coincided with the mass peak M5 and Δ peak D5, signifying the onset of the polymerization process. As the oxidation continued after P5, Ψ decreased slower, as suggested by the reduction in dΨ/dt, to reach the minimum (P6) at +1.0 V. After 1.0 V, beyond P6, Ψ started to increase. There is an inflection around 1.1 V. It appeared in both forward and backward sweeps, suggesting that the presence of the inflection is not an artifact.

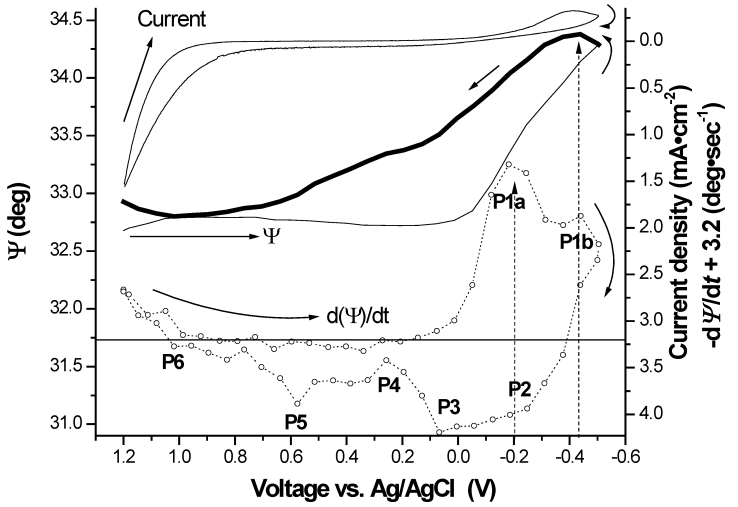

Fig. 5 Progression of ellipsometric angle Ψ during CV sweep and dΨ/dt of cycle 14. The arrows indicate the direction of voltage sweep (in time propagation).

DISCUSSION

The plots of the first derivative of the profiles in mass and ellipsometric angles, dm/dt, dΔ/dt, and dΨ/dt, of cycle 14 are summarized in Fig. 6. A comparison of all three curves indicates that almost all of the underlying processes on the electrode surface, as numbered from 1 to 6, are detected, and the signatures from these processes are shown in all three profiles. This is a validation of the consistency in the results measured in all three experiments in a coherent, synchronized manner.

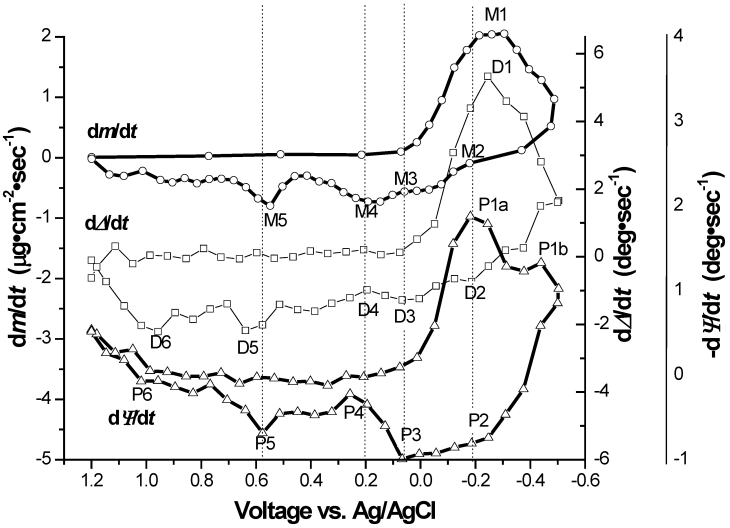

Fig. 6 Mass and ellipsometric angles derivation plots, derivatives as dm/dt, d(Δ)/dt, and d(Ψ)/dt plots of cycle 14.

We should note that the complex relationship in the ellipsometric angles, which gives information on film thickness and, possibly, the chemical nature of the film composition and the change in composition through reactions on the electrode surface. It is also of paramount importance to emphasize that the development of Δ and Ψ, in concert with m, in the forward sweep of the reduction regime, reflects the MG adsorption on the electrode surface, as signified by

- the coherent presence of M1 and D1, indicating that the mass increase was accompanied by a film thickness growth;
- the displacement of peak 1 behind the peaks M1 and D1, indicating that the coherent mass and film thickness increase is not an electrochemical process in nature; and
- the position of P1a seems to coincide with the reflection point on the up-rising profile in dm/dt and dΔ/dt, respectively, before M1 and D1. This observation is consistent with the complimentary nature of Δ and Ψ.

With the confirmation of the adsorption, in addition to the electrochemical reactions (as represented by peak 1) and/or chemical changes, it is critical to realize that there are, at least, an adsorbed and a polymerized film on the electrode surface.

It is also important to point out that both dm/dt and dΔ/dt display an inflection at about –0.36 V in the forward sweep in the reduction regime after M1 and D1, respectively. At the same time, peaks 1 and P1b coincide at the same potential, implying that they are correlated. In other words, peak P1b most likely reflects the occurrence of the reduction reaction, MG → *l*-MG (*leuco*-MG), shown in Fig. 7 (as proposed by Akkermans et al. [27], when cycling the redox couple in the potential range of –0.5 to +0.5 V). It is then interesting to note that peak P1b also coincides with the inflection point on the dΔ/dt profile, as expected from the complimentary nature of Δ and Ψ. It suffices to say that the dΨ/dt profile provides the most intriguing and crucial evidence to separate the adsorption (as represented by the peaks P1a, D1, and M1) from electrochemical reaction (as represented by peaks 1 and P1b).

As the voltammetry continues in the backward sweep, and the potential is swept toward –0.18 V (where M2, D2, and P2 were assigned), the dm/dt, dΔ/dt, and dΨ/dt transitioned at between –0.41 and –0.36 V to opposite signs in their value. This observation reflects what was remarked earlier regarding the inflections and P1b in the reduction regime in the forward sweep. At this point, it signals the end of the reduction process. The fact that m and Δ remain rather constant; i.e., dm/dt and dΔ/dt are close to

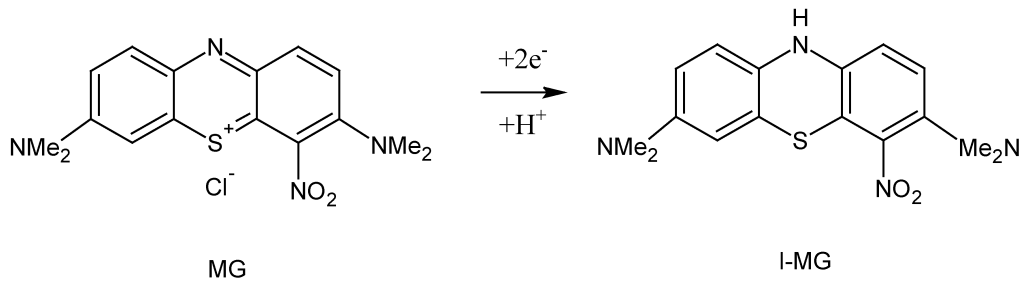

Fig. 7 Proposed redox reaction between MG and *l*-MG by Akkermans et al. [27].

zero, while Ψ decreases with dΨ/dt becomes negative, between –0.41 and –0.26 V, implies that the oxidation of *l*-MG might be triggered as the principal reaction taking place during this time. The peak at D2 signals an on-set of another competing process that begins to cause mass loss from that point onward, as reflected by the shifting of slope in dm/dt and dΨ/dt after M2 and P2. From this point on to M3, D3, and P3 (0.08 V), and further on to M4, D4, and P4 (0.2 V), and M5, D5, and P5 (0.58 V), all three profiles exhibit a consistent pattern of behavior. The trend of changing in value in dm/dt shows the manner of mass being stripped away from the electrode surface. Since the response in the current density was not as fluctuating as in these three profiles, it seems to suggest that the interplay of the oxidation of *l*-MG and desorption of the adsorbed MG layer may be taking place in an ever-changing role in the process. There could be other side reactions involved. Without further study and experimental evidence, it is not clear what was involved in this potential range. It is clear though that M5, D5, and P5 signal the on-set of polymerization of MG.

It should be noted that, without the presence of neutral *l*-MG, the polymerization could not be initiated. This observation was evident in a separate experiment, where we could not obtain any poly-MG film of discernable thickness and quality under a potentiostatic deposition at 1.2 V from the MG solution. Therefore, even the CV process has gone through the oxidation of *l*-MG and stripping of adsorbed MG from the electrode surface, a certain amount of *l*-MG must have survived to contribute to the polymerization process. During this polymerization process, from 0.58 to 1.0 V, the dm/dt shows that unreacted MG continued to be stripped away from the electrode surface. At the same time, the steady dΔ/dt and decreasing dΨ/dt transitions indicate that the poly-MG film starts to form on the surface as well.

Although the above qualitative analysis gave us a very informative understanding of the underlying poly-MG deposition process in the voltammetric cycles, quantitative analysis from the current set of data remains difficult. A major problem arises from the accuracy of the QCM measurements, which are sensitive to the measuring environmental control; for instance, temperature and its variations. Not knowing the confidence interval in the accuracy in QCM, we were not able to conduct any useful quantitative analysis, since doing so can lead to erroneous results in any derived quantity such as density or porosity of the film.

Another problem in correlating the results quantitatively comes from the issue arising from the different spatial basis used to derive the information in different methods. For instance, the electrochemical and microgravimetric measurements are using the entire electrode surface area in gathering the data. The ellipsometric measurements, however, only cover an area as large as 400 by 600 μm to determine the film thickness. There will be a question about the thickness if it were representative. If the film deposition were not homogeneous, we may erroneously use it in subsequent derivations of film property such as density or porosity. We can exemplify this problem by the following case.

When the thickness increase is related to the mass increase measured by the QCM, the resulting density of the poly-MG layer is increased from 5.8 to 8.6 g·cm^{-3} in the four CV cycles shown in this work. Such high values and significant changes within four cycles indicate a problem of the analysis as we explained. The error may also come from the application of Sauerbrey equation in the QCM meas-

urements of poly-MG deposition, due to the propagation of shear acoustic wave in the viscoelastic film [28]. At least, we should measure ellipsometric angles on multiple spots across the sample to minimize the error.

CONCLUSION

An in situ, nondestructive technique, which combines imaging ellipsometry and QCM, was applied with CV for transient study of poly-MG film deposition. From the ellipsometric measurements, we derived the thickness progression of the film growth with nanometer resolution, while the QCM gave us the microgravimetric correlation of the mass change on the electrode surface. With the synchronized spatial, mass and charge correlation, we were able to distinguish certain physical and/or chemical processes, e.g., adsorption/desorption; from electrochemical redox reactions. This approach allows us to derive stepwise information on the underlying processes involved in the polymerization. Although qualitatively useful, we also realized the limitations of this unique approach in providing sufficient accuracy in certain quantitative analysis and derivation of useful film properties such as density or porosity. Combination with other techniques is being considered to resolve this issue in the quantitative analysis.

ACKNOWLEDGMENTS

The authors would like to thank the U.S. Office of Naval Research for the support of this work under the Hawaii Environmental and Energy Technologies (HEET) initiative (Contract No. N0014-01-1-0928; PI: Richard Rocheleau). Their gratitude also goes to Dr. Michael J. Cooney of HNEI and Prof. Plamen Atanassov of the University of New Mexico for their helpful discussions.

REFERENCES

1. A. Hamnett, A. R. Hillman. *Ber. Bunsenges. Phys. Chem.* **91**, 329 (1987).
2. A. Hamnett, A. R. Hillman. *J. Electroanal. Chem.* **233**, 125 (1987).
3. R. Greef, M. Kalaji, L. M. Peter. *Faraday Discuss. Chem. Soc.* **88**, 277 (1989).
4. A. Redondo, E. A. Ticianelli, S. Gottesfeld. *Mol. Cryst. Liq. Cryst.* **160**, 185 (1988).
5. J. Rishpon, A. Redondo, C. Derouin, S. Gottesfeld. *J. Electroanal. Chem.* **294**, 73 (1990).
6. I. Rubinstein, J. Rishpon, E. Sabatani, A. Redondo, S. Gottesfeld. *J. Am. Chem. Soc.* **112**, 6135 (1990).
7. J. Rishpon, S. Gottesfeld. *Biosens. Bioelectron.* **6**, 143 (1991).
8. E. Sabatani, E. Ticianelli, A. Redondo, I. Rubinstein, J. Rishpon, S. Gottesfeld. *Synth. Met.* **55–57**, 1293 (1993).
9. E. Sabatani, A. Redondo, J. Risphon, A. Rudge, I. Rubinstein, S. Gottesfeld. *J. Chem. Soc., Faraday Trans.* **89**, 287 (1993).
10. S. Gottesfeld, Y.-T. Kim, A. Redondo. *Phys. Electrochem.* 393 (1995).
11. T. Tjaernhage, M. Sharp. *Electrochim. Acta* **39**, 623 (1994).
12. E. J. Severin, N. S. Lewis. *Anal. Chem.* **72**, 2008 (2000).
13. T. McMillan, J. E. Rutledge, P. Taborek. *J. Low Temp. Phys.* **138**, 995 (2005).
14. R. P. Richter, A. R. Brisson. *Biophys. J.* **88**, 3422 (2005).
15. L.-C. Xu, C. A. Siedlecki. *Biomaterials* **28**, 3273 (2007).
16. C. Picart, B. Senger, K. Sengupta, F. Dubreuil, A. Fery. *Colloids Surf., A* **303**, 30 (2007).
17. I. Zhitomirsky, A. Hashambhoy. *J. Mater. Process. Technol.* **191**, 68 (2007).
18. C. K. O'Sullivan, G. G. Guilbault. *Biosens. Bioelectron.* **14**, 663 (1999).
19. H. Arwin. "Ellipsometry in life sciences", in *Handbook of Ellipsometry*, Chap. 12, p. 799, William Andrew, Norwich (2005).

20. H. G. Tompkins. *A User's Guide to Ellipsometry*, Academic Press, New York (1993).
21. H. G. Tompkins, W. A. McGahan. *Spectroscopic Ellipsometry and Reflectometry, A User's Guide*, John Wiley, New York (1999).
22. J. F. Rusling, S. L. Suib. *Adv. Mater.* **6**, 922 (1994).
23. G. Sauerbrey. *Z. Phys.* **155**, 206 (1959).
24. V. Svoboda, M. J. Cooney, C. Rippolz, B. Y. Liaw. *J. Electrochem. Soc.* **154**, D113 (2007).
25. D.-M. Zhou, H.-Q. Fang, H.-Y. Chen, H.-X. Ju, Y. Wang. *Anal. Chim. Acta* **329**, 41 (1996).
26. V. Svoboda, M. J. Cooney, B. Y. Liaw, S. Minteer, E. Piles, D. Lehnert, S. C. Barton, D. Ivnitski, P. Atanassov. *Electroanalysis* **20**, 1099 (2008).
27. R. P. Akkermans, S. L. Roberts, F. Marken, B. A. Coles, S. J. Wilkins, J. A. Cooper, K. E. Woodhouse, R. G. Compton. *J. Phys. Chem. B* **103**, 9987 (1999).
28. D. Buttry. "Application of the QCM to electrochemistry", in *A Series of Advances in Electroanalytical Chemistry*, A. J. Bard (Ed.), pp. 23–33, Marcel Dekker, New York (1991).